TAILORING THE DEGRADATION RATE OF MAGNESIUM-LITHIUM ALLOY WITH ALLOYING ELEMENTS OF GADOLINIUM AND NICKEL

Mengyao Pang [a], Tao Zhong [b], Siyuan Jin [a], Xiaochun Ma [a], Ruizhi Wu [a] *, Legan Hou [a] *, Nodir Turakhodjaev [e,f], Sharofuddin Mardonakulov [e],Iya I. Tashlykova-Bushkevich [c], Boris Krit [d], Jinghuai Zhang [a]

[a] Key Laboratory of Superlight Materials & Surface Technology, Ministry of Education, Harbin Engineering University, Harbin 150001, China

[b] Department of Science and Technology, Nanning College for Vocational Technology, Nanning 530008, China

[c] Physics Department, Belarusian State University of Informatics and Radioelectronics, Minsk 220013, Belarus

[d] Moscow Aviation Institute, Russian National Research University, Moscow 121552, Russia

[e] Department of Machine Building, Tashkent State Technical University, Tashkent 100095, Uzbekistan

[f] Uzbek-Japan Innovation Center of Youth, Tashkent 100095, Uzbekistan

1. Introduction

With the depletion of fossil energy sources, oil and gas exploration begins to transform into unconventional oil and gas resources that are difficult to extract with complex storage conditions, lower permeability and less economically efficiency [1]. The fracturing ball is a plugging tool for horizontal wells in the segmented fracturing process [2], and plays a critical role in improving the efficiency of oil and gas production [3]. It requires greater pressure for hydraulic fracturing techniques to obtain oil and in the underground environment the temperature is higher [4]. Fracturing balls always serve in the environment of high-temperature and high-pressure [5], in which it is required that fracturing balls possess both high strength and high corrosion rate simultaneously [6]. It is easier for the lower density fracturing ball to follow the fracking fluid into the ball seat [7]. Fracturing balls need lightweight that can withstand the high pressure, high temperature and have rapid corrosion rate during fracturing process.

Currently, extensive investigations are being conducted on various magnesium alloy fracking ball materials systems, such as magnesium-aluminum (Mg-Al) alloy [8], magnesium-zinc (Mg-Zn) alloy [9] and Mg-rare earth (RE) alloy [10]. However, the prioritization of density requirements for fracturing balls has been relatively low. Doping with high levels of other elements leads to a further increase in density. Magnesium-lithium (Mg-Li) alloy possesses the lowest density among metallic engineering materials, with a density of 1.4-1.6 g/cm^3 [11]. Besides the low density, Mg-Li alloy also has the characteristics of high specific strength, poor corrosion resistance etc. [12]. The poor corrosion resistance of Mg-Li alloy limits its applications as engineering materials. However, poor corrosion resistance makes

it good for biomedical applications [13] and fracturing balls [14]. Due to the lower potential of Li, the degradation rate of Mg-Li alloy is often much higher than that of other Mg alloys [11]. Adjusting the galvanic coupling corrosion between the second phase and matrix can improve the corrosion rate [15]. Now, research on Mg-Li alloys for fracturing balls remains a gap.

2. Experimental

Mg-8Li-4Gd-*x*Ni (*x* = 0, 0.5, 1, 1.5 wt.%) alloys were prepared in a vacuum induction melting furnace protected by argon atmosphere. The materials used are pure Mg (99.9 wt.%), pure Li (99.9 wt.%), master alloys of Mg-30 wt.% Gd and Mg-30 wt.% Ni. The microstructure of the alloy was observed by optical microscope (OM), and the morphology of the alloy before and after corrosion was analyzed by scanning electron microscope (SEM) and energy dispersive spectrometer (EDS). The microstructure of the alloy was also characterized by transmission electron microscope (TEM). X-ray diffraction (XRD) was used for phase composition analysis, and X-ray photoelectron spectroscopy (XPS) was used to analyze the surface chemical properties of the corroded samples. The Volta potential fluctuation and surface morphology with different microstructures was measured by means of atomic force microscope (AFM).

Electrochemical analysis and hydrogen evolution were used to research the corrosion behavior of Mg-Li-Gd-Ni alloys. Electrochemical tests were performed using a three-electrode system with a platinum electrode as counter electrode, a saturated calomel electrode as reference electrode and the sample with an exposed surface area of 1 cm^2 as the working electrode. The frequency range for electrochemical impedance spectroscopy (EIS) tests was set to 100 kHz ~ 100 MHz with an interference signal of 10 mV, and the tests were performed at room temperature. Hydrogen evolution was performed using glass devices including beakers, droppers and funnels for hydrogen collection and volume measurements, and samples were immersed in 3.0 wt.% KCl solution for 8 hours at room temperature to measure the weight loss rate and washed for 5 min using 200 g/L CrO_3 + 10 g/L $AgNO_3$ solution at the end of the test for the corrosion surface observation [28].

3. Results and Discussion

3.1. Microstructure characterization

The XRD patterns of Mg-Li-Gd-Ni alloys with different Ni contents are shown in Figure 1. Mg-Li-Gd-Ni alloys are composed of α-Mg, β-Li, LPSO, Mg_3Gd and $GdNi_3$ phases. With the increase of Ni content, the amount of α-Mg and Mg_3Gd decreases, and the amount of $GdNi_3$ increases. Figure 2 shows the optical microstructure of the Mg-Li-Gd-Ni alloys. Gd-rich particles are dispersed in the Mg-Li alloy. When Ni is added to the Mg-Li alloy, α-Mg is mainly distributed at the grain boundaries and a few parts inside the grains. LPSO appears in α-Mg, the content of LPSO increases first and then decreases.

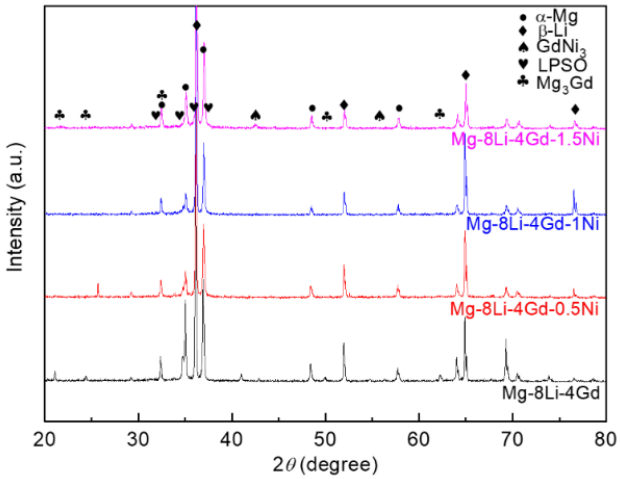

Figure 1. XRD diffractograms of Mg-8Li-4Gd-*x*Ni (*x* = 0, 0.5, 1, 1.5 wt.%) alloy.

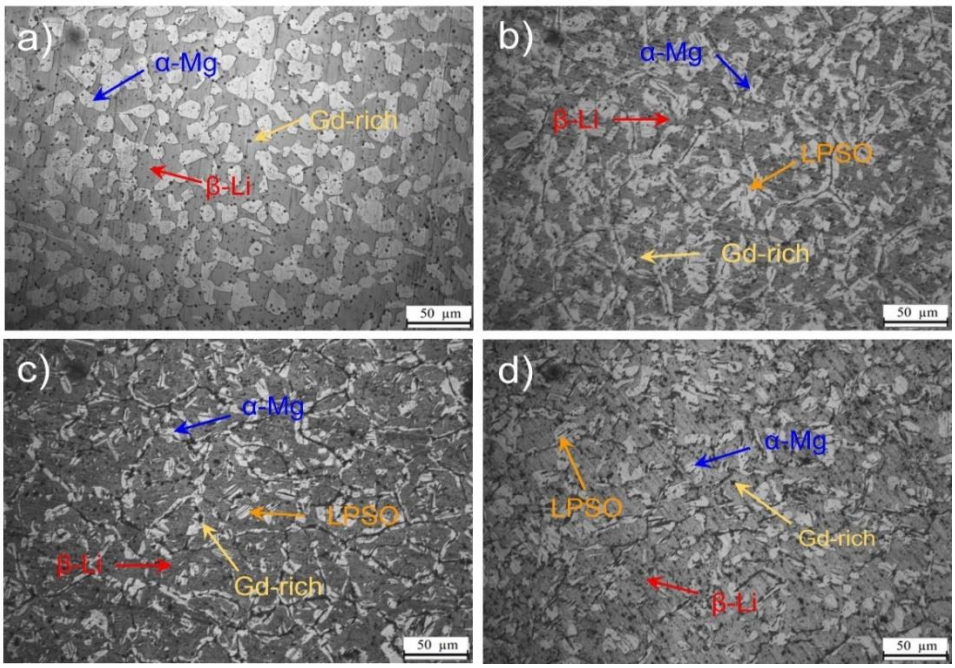

Figure 2. Optical microstructure of the Mg-8Li-4Gd-*x*Ni alloys: a) *x* = 0wt.%; b) *x* = 0.5 wt.%; c) *x* = 1 wt.%; d) *x* = 1.5 wt.%.

SEM observations and EDS results are performed on the Mg-Li-Gd-Ni alloy, as shown in Fig. 3. The bright particles in the Mg-8Li-4Gd alloy are Mg_3Gd phase, EDS results prove the presence of more Gd and Mg in the particles. After the addition of Ni, more lamellar secondary phases exist in the α-Mg and grow into thick and compact plates. EDS results show a typical LPSO phase. The continuous network is disrupted, and intermittent and blocky LPSO appears with Ni content. Meanwhile, the mount of Gd-rich phase increases and the Gd-rich regions with high Ni content appear, presumably as $GdNi_3$ phase.

4. Conclusions

(1) The addition of Ni results in the formation of 24R structured LPSO and

$GdNi_3$ phases. With the increase of Ni content, the morphology of LPSO changes from continuous to intermittent. Higher fault energy makes LPSO difficult to form when the atomic ratio of Gd to Ni is lower than 4:3.

(2) Mg-8Li-4Gd-1.5Ni alloy shows a very high corrosion rate, with the weight loss rate and hydrogen precipitation rate of 0.36 mg/cm^2·min and 0.37 mL/cm^2·min, which is 75 times higher than that of Mg-8Li-4Gd alloy. The addition of positive potential Ni to the alloy leads to an increase in the potential difference. The number of galvanic corrosion sites increase caused by intermittent network LPSO.

(3) The corrosion of Mg-Li-Gd-Ni alloy is mainly galvanic corrosion, and the corrosion formation is mainly due to the formation of potential difference between the second phase and the matrix. With the increase of Ni content, galvanic corrosion effect between the bulk LPSO/$GdNi_3$ and α-Mg/β-Li matrix is increased, resulting in a significantly higher corrosion rate of the alloy.

References

[1] O. Tavakkoli, H. Kamyab, R. Junin, V. Ashokkumar, A. Shariati, SDS−aluminum oxide nanofluid for enhanced oil recovery: IFT, adsorption, and oil displacement efficiency, ACS Omega 7(2022) 14022-14030.

[2] O. Tavakkoli, H. Kamyab, M. Shariati, A. M. Mohamed, R. Junin, Effect of nanoparticles on the performance of polymer/surfactant flooding for enhanced oil recovery: A review, Fuel 312 (2022) 122867.

[3] J. Sun, W. B. Du, J. J. Fu, K. Liu, S. B. Li, Z. H. Wang, H. X. Liang, A review on magnesium alloys for application of degradable fracturing tools, J. Magnes. Alloy. 10(10) (2022) 2649-2672.

[4] J. F. Wang, S. Q. Gao, X. Y. Liu, X. Peng, K. Wang, S. J. Liu, W. Y. Jiang, S. F. Guo, F. S. Pan, Enhanced mechanical properties and degradation rate of Mg-Ni-Y alloy by introducing LPSO phase for degradable fracturing ball applications, J. Magnes. Alloy. 8(1) (2020) 127-133.

[5] H. Y. Niu, K. K. Deng, K. B. Nie, F. F. Cao, X. C. Zhang, W. G. Li, Microstructure, mechanical properties and corrosion properties of Mg-4Zn-xNi alloys for degradable fracturing ball applications, J. Alloys Compd. 787 (2019) 1290-1300.

[6] X. Peng, W. C. Liu, G. H. Wu, Strengthening-toughening methods and mechanisms of Mg-Li alloy: a review, Rare Metals 41(4) (2022) 1176-1188.

[7] L. Liu, S. R. Yu, Y. F. Niu, E. Y. Liu, Preparation and properties of hollow glass microspheres reinforced Mg alloy degradable composites, J. Alloys Compd. 835 (2020) 155198.

[8] D. W. Wang, K. J. Dong, Z. Z. Jin, K. Guan, F. Y. Cao, H. Zhao, M. Zha, H. Y. Wang, Novel Mg-Al-Sn-Ca with enhanced mechanical properties and high corrosion rate via sub-rapid solidification for degradable magnesium alloy.